Far infrared vibration-rotation-tunneling spectroscopy and internal dynamics of methane–water: A prototypical hydrophobic system

L. Dore,[a] R. C. Cohen,[b] C. A. Schmuttenmaer,[c] K. L. Busarow, M. J. Elrod, J. G. Loeser, and R. J. Saykally
Department of Chemistry, University of California, Berkeley, California 94720

(Received 26 March 1993; accepted 1 October 1993)

Thirteen vibration-rotation-tunneling (VRT) bands of the CH_4–H_2O complex have been measured in the range from 18 to 35.5 cm^{-1} using tunable far infrared laser spectroscopy. The ground state has an average center of mass separation of 3.70 Å and a stretching force constant of 1.52 N/m, indicating that this complex is more strongly bound than Ar–H_2O. The eigenvalue spectrum has been calculated with a variational procedure using a spherical expansion of a site–site *ab initio* intermolecular potential energy surface [J. Chem. Phys. **93**, 7808 (1991)]. The computed eigenvalues exhibit a similar pattern to the observed spectra but are not in quantitative agreement. These observations suggest that both monomers undergo nearly free internal rotation within the complex.

I. INTRODUCTION

Water–hydrophobe interactions govern essential features of many chemical and biochemical processes. Considerable controversy exists in the literature concerning the correct molecular description of the macroscopic phenomena commonly associated with hydrophobic interactions (e.g., phase separation of oil and water, micelle formation, tertiary protein structure),[1–3] and the lack of accurate intermolecular potentials for describing the interaction of water with "hydrophobic" molecules certainly constitutes an impediment to this endeavor. Recent studies of the prototypical system Ar–H_2O (Refs. 4 and 5) represent the initial phase of ongoing efforts in this laboratory to obtain accurate experimental potentials for describing hydrophobic interactions. Numerous vibration-rotation-tunneling (VRT) states of several isotopes were measured by tunable far infrared laser spectroscopy of Ar–H_2O clusters formed in a cw planar supersonic expansion. These data were then used in a direct nonlinear least-squares fit to determine the full three-dimensional anisotropic intermolecular potential surface (IPS) describing the interaction of an Ar atom with water.[6,7]

The results of the Ar–H_2O studies provide the framework in which to interpret and understand the spectra and dynamics of more complicated systems, such as CH_4–H_2O. The CH_4–H_2O complex is the simplest hydrocarbon–water cluster, and is closely related to Ar–H_2O since the charge distribution of the methane is almost spherical, with the octopole as the lowest nonvanishing multipole moment. Therefore, in CH_4–H_2O only high order terms in the multipole expansion of the electrostatic interaction (octopole–dipole, hexadecapole–dipole, ...) are present; thus the spectra of this complex probe the importance of these higher order terms in the IPS, whereas they are usually neglected when the more typical low order terms are present.

This study and the accompanying microwave (MW) work[8] constitute the first spectroscopic studies of this cluster; in fact it is only within the last 3 years that any high resolution spectra for methane containing complexes have been reported. Legon and co-workers have studied dimers of the type CH_4–HX [X=F (Ref. 9), Cl (Ref. 9), CN (Refs. 10, 11), Br (Ref. 12)] and Ohshima and Endo have investigated the internal dynamics of methane within the CH_4–HCl complex.[13] These studies indicate that methane acts as a proton acceptor. However, microwave spectra probe only the average structure in a given VRT state (usually the ground state), and do not necessarily yield structures that have any fundamental relationship to the intermolecular forces acting in the system. This has been shown, for example, in the cases of the Ar–H_2O (Refs. 6, 7) and Ar–NH_3 (Ref. 14) complexes.

Theoretical studies of the CH_4–H_2O complex have been carried out,[15–17] but there are serious discrepancies among the results. The *ab initio* calculations of Szczęśniak *et al.*[15] support previous theoretical results of Novoa *et al.*,[16] indicating that the global minimum occurs indeed at the C···H–O contact. On the contrary, the global minimum configuration found by Woon *et al.*,[17] in their *ab initio* study, occurs at the C–H···O contact.

Tunable far-infrared (FIR) laser spectroscopy has been used to obtain the first high resolution VRT spectrum of CH_4–H_2O produced in a cw planar supersonic jet. Six bands with origins between 18 and 19 cm^{-1} and seven bands with origins in the range 25.5–35.5 cm^{-1} have been rotationally assigned. The bands sample 13 different VRT levels as upper states, and 8 levels as lower states, which match the observed MW data.[8] The slow interconversion of different nuclear spin conformers in the supersonic expansion leads to population of at least six different VRT levels of the complex, and the observed high vibrational level density is the result of the slightly hindered internal motion of both monomers within the cluster.

The CH_4–H_2O system is much more complicated than

[a]Permanent address: Dipartimento di Chimica "G. Ciamician," Università di Bologna, via Selmi 2, 40136 Bologna, Italy.
[b]Present address: Department of Chemistry, Harvard University, Cambridge, Massachusetts 02138.
[c]Present address: Department of Chemistry, University of Rochester, Rochester, New York 14627.

 0021-9606/94/100(2)/863/14/$6.00

TABLE I. FIR laser lines used in the present study.

Lasing gas	Frequency (GHz)
DCOOD	527.9260
HCOOH	584.3882
HCOOH	692.9514
HCOOH	761.6083
HCOOD	849.8280
CH_3OD	939.4940
CH_3OD	980.5916
CH_3OD	1016.8972
CH_2F_2	1042.1504
CH_2DOH	1101.1594

any other system for which an anisotropic IPS has been experimentally determined. Detailed experimental intermolecular potential surfaces have been developed for several two-dimensional systems [Rg–H_2 (Ref. 18), Rg–HX, X=halogen (Ref. 19)], for the three-dimensional system Ar–H_2O,[6,7] and for the (quasi) four-dimensional system Ar–NH_3.[14] The high symmetry of the CH_4–H_2O cluster, compared to $(H_2O)_2$, makes investigation of the IPS a reasonable starting point for the development of general methods for treating the pairwise interactions of polyatomic molecules, such as the water dimer. Nevertheless, significant advances in computational approaches for determining the eigenvalues of strongly coupled multidimensional systems are still required before a parametrized six-dimensional IPS can actually be determined from the experimental data.

In this work we perform approximate calculations to obtain the bending VRT levels of the complex, using the site–site potential of Woon *et al.*[17] expanded in products of Wigner rotation matrices. A comparison of these results to the experimental data indicates that either a less approximate method or a more reliable potential surface, or both, will be required to obtain a quantitative agreement between theory and experiment.

II. EXPERIMENT

Both the tunable FIR laser system and the planar supersonic jet have been described in detail previously.[20,21] Tunable FIR radiation is generated by mixing the output of a narrow band (<100 kHz), fixed frequency, optically pumped FIR laser with the output of a MW synthesizer or its harmonics in a Schottky barrier diode. The tunable radiation is separated from the fixed frequency carrier with a polarizing Michelson interferometer, and then directed to multipass optics enclosing the planar supersonic expansion. The radiation, detected by a Putley mode InSb detector, is monitored via lock-in detection at $2f$. In this study the fixed frequency radiation was provided by the laser lines reported in Table I.

Clusters of CH_4–H_2O were generated by flowing argon over water and mixing the resulting Ar/H_2O mixture with methane in a 5:1 ratio. The composition of the mixture was controlled using MKS flow controllers. The $Ar/CH_4/H_2O$ mixture was expanded continuously through a 100×0.025 mm slit into a chamber maintained at 250 mTorr by a 1200 ℓ/s Roots system.

We have scanned from 500 to 1125 GHz. The coverage is almost continuous above 900 GHz, but not below this frequency. Background subtraction has been implemented by taking two scans and turning off the CH_4 in the second one; in this way only spectral features requiring CH_4 have been observed. In all, 950 peaks have been recorded, and we have been able to give an unambiguous rotational assignment for 329 of them, as described in the following sections.

III. SYMMETRY

The experimental data allow rigorous assignment of the total angular momentum (J), its projection (Ω) along the van der Waals (vdW) axis, and the relative parity of connected states. The molecular symmetry (MS) group of CH_4–H_2O will be used for identification and labeling of the observed VRT energy levels and to determine the optical selection rules. The MS group is the set of the feasible nuclear permutations, that is, the feasible nuclear permutation group, plus the products of these operations with the space-fixed inversion operator; by a feasible permutation one means an interchange of the hydrogen nuclei of the cluster that lead to a structure which is separated from the initial structure by an accessible potential barrier.

If methane and water are assumed to be nearly free internal rotors within the complex, the MS group for the cluster is the direct product of three groups, the nuclear permutation groups of the two monomers (because all permutations are possible), and a group, isomorphic to C_S, formed by identity and inversion operations (this preserves the handedness of the methane). This group is designated G_{48} and its character table is given by Bunker,[22] and is reproduced in Table II. The numbers 1–4 represent CH_4 hydrogens and the letters a and b represent H_2O hydrogens. The labels describing the irreducible representations of G_{48} can be understood by considering a direct product wave function $\psi_{CH_4}\otimes\psi_{H_2O}\otimes\psi_{e\text{-}o\text{-}e}$. The letters A, E, and F indicate the degeneracy of the state as well as the symmetry of the internal functions (ψ_{CH_4}) which describe the motions of the CH_4 monomer within the molecule. The superscripts $\pm$ refer to the symmetric/antisymmetric property of the internal rotation functions of the H_2O subunit (ψ_{H_2O}) with respect to interchange of the hydrogens; the symmetric para states are labeled Γ^+, while the ortho states are of Γ^- symmetry. Finally, the subscripts 1 and 2 refer to the symmetry of the state with respect to the parity operator. The overall parity depends on the parity of ψ_{CH_4}, ψ_{H_2O}, and on the parity of the overall end-over-end rotational function $\psi_{e\text{-}o\text{-}e}$.

An electric dipole allowed transition connects only states with the same methane and water symmetry, but with opposite overall parity, because of the antisymmetric behavior of the dipole operator with respect to the space inversion. Note from the character table that for states of E symmetry the two parities are degenerate (no subscripts

TABLE II. Molecular symmetry group for the CH_4–H_2O dimer.

G_{48}	E 1	(123) 8	(14)(23) 3	(1423)(ab) 6	(23)(ab) 6	(ab) 1	(123)(ab) 8	(14)(23)(ab) 3	(1423) 6	(23) 6
A_1^+	1	1	1	1	1	1	1	1	1	1
A_2^+	1	1	1	−1	−1	1	1	1	−1	−1
E^+	2	−1	2	0	0	2	−1	2	0	0
F_1^+	3	0	−1	1	−1	3	0	−1	1	−1
F_2^+	3	0	−1	−1	1	3	0	−1	−1	1
A_1^-	1	1	1	1	1	−1	−1	−1	−1	−1
A_2^-	1	1	1	−1	−1	−1	−1	−1	1	1
E^-	2	−1	2	0	0	−2	1	−2	0	0
F_1^-	3	0	−1	1	−1	−3	0	1	−1	1
F_2^-	3	0	−1	−1	1	−3	0	1	1	−1

are required). This fact will be useful in determining the symmetry of states with nonzero vibrational angular momentum; such states having $\Omega > 0$, but with no observable splitting between the two different parity components, will be assigned to E symmetry. The states that have observable parity doubling cannot be of E symmetry, but it is impossible to rigorously distinguish between either A or F symmetry, thus these states will be designated as A/F. Experimental measurement of the small hyperfine structure associated with the hydrogen nuclei in this cluster could be used to confirm the symmetries of the CH_4 and H_2O internal rotor wave functions, and thereby the overall symmetries of the VRT states, but the resolution required for this kind of measurement is beyond the capabilities of our instrument.

IV. RESULTS

Extensive scannings have been carried out in order to observe all the eight lower states reported in the MW work.[8] Thirteen different VRT bands have been assigned in all. The assigned lines have been fit to a standard pseudodiatomic Hamiltonian

$$E = \nu_0 + B[J(J+1)] - D_J[J(J+1)]^2 + H_J[J(J+1)]^3 + \cdots \pm \tfrac{1}{2}\{q[J(J+1)] - q_d[J(J+1)]^2 + q_h[J(J+1)]^3 + \cdots\}. \quad (1)$$

The l-type doubling constants (q) characterize the difference in rotational energy levels for (+) and (−) parity states with $\Omega > 0$, the degeneracy of which is lifted by Coriolis coupling. A minus sign in the l-type doubling term of Eq. (1) is used for the component having the same vibrational ($\psi_{CH_4} \otimes \psi_{H_2O}$) symmetry as the other state connected by the VRT band, and a plus sign is used for the opposite parity component. For example, consider a VRT band connecting a $\Omega > 0$ VRT state to a second state. If q is determined to be *positive*, there are two alternative scenarios, (i) the state perturbing the $\Omega > 0$ state is *higher* in energy and pushes down the component having the same parity; this lower energy component has the same parity of the second state involved in the transition, hence the perturbing state and the second state have the *same* parity; (ii) the perturbing state is *lower* in energy than the $\Omega > 0$ state and pushes up the same parity component; since this higher energy component has opposite parity with respect to the second state, the perturbing state and the second state have *opposite* parity. The reverse holds for *negative* q values.

Bands having a common lower state have been fit simultaneously. The observed frequencies along with the residuals and the spectroscopic parameters (1σ uncertainties) determined from the fit are reported in Tables III–X. A vibrational state is labeled as Σ, Π, Δ according to the value of the angular momentum projection quantum num-

TABLE III. Observed frequencies (MHz), residuals (MHz), and spectroscopic constants from a joint fit of the $(E)_1$ and $(E)_2$ bands.

Bands $J' \leftarrow J''$	$(E)_1$ Observed	$(E)_1$ O–C	$(E)_2$ Observed	$(E)_2$ O–C
	Σ←Π		Δ←Π	
6 7	481 374.8	1.0		
5 6	489 968.0	−0.1	491 812.8	1.1
4 5	498 551.3	−0.2	500 194.5	0.0
3 4	507 126.1	0.7	508 622.8	−0.9
2 3	515 692.7	0.3	517 092.8	0.2
1 2	524 254.1	−0.4		
0 1	532 812.0	−0.9		
1 1	541 359.5	−0.5		
2 2	541 344.3	0.0	542 744.8	0.3
3 3	541 316.1	−0.1	542 813.7	−0.7
4 4	541 270.3	−0.6	542 913.4	−0.5
5 5	541 202.2	−1.4	543 047.3	0.2
6 6	541 110.2	0.1	543 218.1	0.6
7 7	540 989.1	0.4	543 426.3	−0.3
8 8	540 841.2	−0.3	543 672.0	−1.2
2 1	558 451.2	1.4	559 850.8	0.8
3 2	566 969.4	1.3	568 466.5	0.2
4 3	575 461.4	−0.3	577 104.3	−0.4
5 4			585 765.8	−0.8
6 5	592 344.8	−0.8	594 453.3	0.4
7 6	600 725.4	0.4	603 163.2	0.3
8 7			611 893.0	0.4
9 8			620 633.9	0.3
B'' (MHz)	4277.222(42)			
D_J'' (kHz)	105.56(56)			
ν_0 (MHz)	541 366.88(44)		542 679.10(67)	
B' (MHz)	4273.951(72)		4287.728(81)	
D_J' (kHz)	189.7(22)		37.6(19)	
H_J' (Hz)	393.(21)		−306.(13)	

TABLE IV. Observed frequencies (MHz), residuals (MHz), and spectroscopic constants from a joint fit of the $(A/F)_1$ and $(A/F)_3$ bands.

Bands $J' \leftarrow J''$	$(A/F)_1$		$(A/F)_3$			
	Observed	O–C	Observed	O–C	Observed	O–C
	$\Sigma \leftarrow \Pi$			$\Delta \leftarrow \Pi$		
8 9					486 936.2	0.1
7 8			494 614.3	2.4	495 465.4	−0.1
6 7			503 221.5	−1.6	504 026.7	0.1
5 6	494 783.2	−0.5	511 881.5	3.7	512 617.0	0.5
4 5	503 449.3	−0.7	520 597.4	−0.9	521 232.2	0.3
3 4	512 123.4	−0.2	529 371.5	−5.2		
2 3	520 805.1	0.2	538 188.3	−0.6	538 527.1	−0.5
1 2	529 495.8	2.1				
0 1	538 189.8	0.9				
1 1	546 831.5	0.8				
2 2	546 715.2	0.2	564 637.3	4.3	564 437.7	0.0
3 3	546 540.9	−1.4	564 733.1	−1.0	564 288.3	−0.3
4 4	546 311.9	−1.9	564 910.3	3.3	564 095.3	−0.4
5 5	546 029.1	−2.0			563 863.4	−0.5
6 6	545 695.1	−0.9			563 599.1	−0.2
7 7	545 312.0	1.3			563 309.9	0.4
8 8	544 880.4	2.4			563 003.5	0.4
9 9	544 402.0	1.1				
10 10	543 880.7	−2.0				
2 1	564 291.7	0.4	581 971.4	1.3	582 013.5	−0.5
3 2	572 986.5	0.1	590 640.5	−3.6	590 733.7	0.9
4 3	581 669.9	−1.3	599 325.8	0.1	599 454.0	0.9
5 4	590 339.8	−0.0	608 034.6	3.0	608 173.2	0.6
6 5	598 986.2	0.3	616 758.0	−4.1	616 888.8	−0.5
7 6	607 602.8	0.6	625 486.3	−1.0	625 599.9	−1.1
8 7	616 181.2	0.5				
9 8	624 712.3	−0.1				
B'' (MHz)	4365.225(47)		4365.225[a]			
D_J'' (kHz)	131.95(47)		131.95[a]			
q'' (MHz)	30.152(26)		30.152[a]			
q_D'' (kHz)	48.18(38)		48.18[a]			
ν_0 (MHz)	546 888.76(45)		564 562.3(45)		564 590.43(72)	
B' (MHz)	4351.239(50)		4359.13(66)		4354.532(68)	
D_J' (kHz)	140.28(51)		−384(25)		104.35(84)	
H_J' (kHz)			−3.94(28)			

[a]Fixed to the value obtained by a joint fit of the $\Sigma \leftarrow \Pi$ band and the second $\Delta \leftarrow \Pi$ subband. See text.

ber Ω. The value of Ω is assigned based on the lowest J value present in the rotational manifold (because $J \geqslant \Omega$). As previously noted, a state is assigned as having E symmetry if there is no parity doubling or as A/F otherwise. A subscript is used to label different bands with the same symmetry. In some cases a sextic distortion constant is introduced in order to obtain a better fit. It should be noted that this additional constant is likely to account for a Coriolis perturbation, and has no mechanical significance. The results obtained in this way are identical to the results of fitting combination differences for the lower and upper state separately.

In the case of an A/F symmetry $\Omega \geqslant 1 \leftarrow \Omega \geqslant 1$ band, two subbands are observed since both the lower and upper states are parity split. The two columns in Tables IV and IX under the heading $\Delta \leftarrow \Pi$ refer to the two subbands for bands $(A/F)_3$ and $(A/F)_7$, respectively. The $(A/F)_6$ band in Table IX has been assigned by lower state combination differences and shares this state with the $(A/F)_7$ band. Because the upper state is strongly perturbed, the lower constants have been fixed to values obtained from the $(A/F)_7$ band fit and results of separate fits for each band are reported. In Table IV the upper state of the first $\Delta \leftarrow \Pi$ subband of the $(A/F)_3$ band is perturbed, thus this subband has been fit constraining the lower state spectroscopic constants to the values obtained from a joint fit of the $\Sigma \leftarrow \Pi$ band and of the other $\Delta \leftarrow \Pi$ subband.

Figures 1(a) and 1(b) present an overview of the experimentally determined VRT energy differences in CH_4–H_2O. The eight lower states are all reported at zero energy because there is no experimental constraint on their relative energy separations. The observed states are tentatively grouped as having either ortho or para symmetry with respect to water, based on the assumption that the CH_4 subunit experiences a fairly isotropic potential. Thus, we will employ an Ar–H_2O-like energy level structure[7] complicated by the CH_4 internal dynamics. The CH_4–H_2O bands observed in the 18–19 cm^{-1} region correlate to the $n=0$ $\Pi(1_{10}) \leftarrow \Sigma(1_{01})$ transition of Ar–H_2O occurring at 21 cm^{-1}; the bands observed in the 24–35 cm^{-1} region

TABLE V. Observed frequencies (MHz), residuals (MHz), and spectroscopic constants from a fit of the $(A/F)_2$ band.

Band $J' \leftarrow J''$		$(A/F)_2$ Observed	O–C
		$\Pi \leftarrow \Sigma$	
9	10	471 434.8	0.6
7	8	487 446.9	−0.9
6	7	495 545.7	−0.8
5	6	503 705.4	0.0
4	5	511 924.2	0.2
3	4	520 201.9	0.3
2	3	528 539.0	1.3
1	2	536 931.0	−0.4
6	6	553 731.1	−0.3
5	5	553 795.2	1.2
4	4	553 839.0	−1.2
3	3	553 867.1	−1.2
2	2	553 883.6	1.7
1	1	553 888.4	1.9
1	0	562 445.5	−0.8
2	1	571 055.5	−1.4
3	2	579 715.0	−1.8
4	3	588 422.7	−0.8
5	4	597 175.1	0.8
6	5	605 968.2	1.9
7	6	614 798.3	1.5
8	7	623 661.4	−1.8
B'' (MHz)		4252.899(92)	
D_J'' (kHz)		69.58(90)	
ν_0 (MHz)		553 887.28(98)	
B' (MHz)		4266.23(20)	
D_J' (kHz)		143.(11)	
H_J' (kHz)		0.59(16)	
q' (MHz)		−26.93(27)	
q_D' (kHz)		121.(19)	
q_H' (kHz)		1.14(31)	

TABLE VI. Observed frequencies (MHz), residuals (MHz), and spectroscopic constants from a fit of the $(A/F)_4$ band.

Band $J' \leftarrow J''$		$(A/F)_4$ Observed	O–C
		$\Pi \leftarrow \Sigma$	
10	11	473 064.0	−0.2
8	9	489 414.0	0.7
7	8	497 684.0	−0.1
6	7	506 015.7	−0.1
5	6	514 406.0	−0.3
4	5	522 852.6	−0.4
3	4	531 353.5	−0.1
2	3	539 905.4	−0.1
1	2	548 506.7	0.4
7	7	564 408.9	0.1
6	6	564 773.2	0.1
5	5	565 082.1	−0.4
4	4	565 337.9	−0.3
3	3	565 541.5	0.1
2	2	565 694.1	1.1
1	1	565 794.7	1.0
1	0	574 574.9	−0.6
2	1	583 344.0	−1.3
3	2	592 150.2	−0.3
4	3	600 988.7	0.4
5	4	609 856.2	0.2
6	5	618 750.8	0.3
7	6	627 668.6	−0.3
B'' (MHz)		4345.533(40)	
D_J'' (kHz)		111.45(45)	
ν_0 (MHz)		565 843.93(26)	
B' (MHz)		4343.220(48)	
D_J' (kHz)		117.14(66)	
q' (MHz)		−45.569(30)	
q_D' (kHz)		7.54(65)	

correlate to an Ar–H_2O transition originating from the para ground state $\Sigma(0_{00})$. (The quantum numbers in parentheses refer to the water rotational level from which the vibrational level arises, and n refers to the number of quanta in the intermolecular stretching coordinate.)

A. Ortho states

The two VRT bands with origins at 18.06 and 18.10 cm^{-1} [$(E)_1$ and $(E)_2$, respectively] originate in the same Π state, as evidenced by lower state combination differences. The first one is a $\Sigma \leftarrow \Pi$ band, confirmed by the presence of $P(1)$ and $Q(1)$, and the second one is a $\Delta \leftarrow \Pi$ band, because $Q(1)$ and $P(2)$ are absent. No resolvable parity doubling is present in either band, indicating that the states are of E symmetry.

A second pair of bands which also share a Π lower state are found at 18.24 and 18.83 cm^{-1} [$(A/F)_1$ and $(A/F)_3$, respectively]. The first one is a $\Sigma \leftarrow \Pi$ band and the second one is a $\Delta \leftarrow \Pi$ band. The Π state is parity split with a positive l-type doubling constant of 30.15 MHz, so these states are labeled as A/F. The upper Δ state is also parity split, and the component of opposite parity with respect to the Σ upper state is perturbed, as shown by the negative value of D_J and large residuals.

Finally, two $\Pi \leftarrow \Sigma$ bands at 18.48 and 18.87 cm^{-1} [$(A/F)_2$ and $(A/F)_4$, respectively] have been observed. For both Π upper states the q constants are negative, indicating that in each case the perturbing state is either of opposite parity to the Σ state and above the Π state, or of the same parity of the Σ state and below the Π state.

For all the six observed VRT bands the difference between the upper and the lower state rotational constants is $<0.3\%$, suggesting that the two states accessed by each band sample a similar range of the radial coordinate.

B. Para states

The VRT bands with widely ranging band origins tentatively assigned as connecting para states are E symmetry bands. In fact the $\Sigma \leftarrow \Pi$ band at 24.73 cm^{-1}, the $\Delta \leftarrow \Pi$ band at 27.40 cm^{-1}, and the $\Pi \leftarrow \Pi$ band at 35.29 cm^{-1} [$(E)_3$, $(E)_4$, and $(E)_5$, respectively] all share the same Π lower state, which seems to sample the same radial region as the E ortho states, as evidenced by their nearly identical rotational constants.

The pattern of the remaining bands in the region 28–31 cm^{-1} is similar to that of the A/F ortho transitions. Two bands at 30.25 ($\Sigma \leftarrow \Pi$) and 30.45 ($\Delta \leftarrow \Pi$) cm^{-1} [$(A/F)_6$ and $(A/F)_7$, respectively] sharing the same Π lower state have been observed. The Σ upper state of the former band is strongly perturbed, as shown by the large value of the

TABLE VII. Observed frequencies (MHz), residuals (MHz), and spectroscopic constants from a joint fit of the $(E)_3$, $(E)_4$, and $(E)_5$ bands.

Bands $J' \leftarrow J''$	$(E)_3$		$(E)_4$		$(E)_5$	
	Observed	O–C	Observed	O–C	Observed	O–C
	$\Sigma \leftarrow \Pi$		$\Delta \leftarrow \Pi$		$\Pi \leftarrow \Pi$	
6 7	677 612.1	0.8			996 711.1	−0.4
5 6	687 141.0	−0.6			1 005 661.6	−0.8
4 5	696 511.2	−0.0	778 604.7	0.9		
3 4	705 721.0	0.3	787 213.0	0.8	1 023 369.4	−0.3
2 3	714 768.7	−1.1	795 811.6	0.5	1 032 126.9	−0.6
1 2	723 657.8	−0.1				
13 13			819 313.8	−1.3		
12 12			819 714.4	1.1		
11 11			820 057.9	0.9	1 052 862.0	−1.5
10 10			820 352.6	0.8	1 053 798.3	1.1
9 9	733 215.1	−0.2	820 603.0	−0.1	1 054 621.3	1.6
8 8	734 795.7	0.1	820 814.9	−0.7	1 055 340.0	1.5
7 7	736 186.0	0.1	820 992.1	−1.5	1 055 961.1	0.7
6 6	737 391.3	0.1	821 139.2	−1.8	1 056 491.0	−0.5
5 5	738 414.8	−1.3	821 260.9	−0.3	1 056 936.1	−0.8
4 4	739 263.4	−0.9	821 356.4	−0.5	1 057 300.4	−0.7
3 3	739 939.2	0.1	821 430.1	−0.5	1 057 588.8	0.8
2 2	740 443.2	0.3	821 483.9	−0.3	1 057 801.7	1.1
1 1	740 778.1	0.4			1 057 943.1	2.1
0 1	732 385.1	1.5				
2 1	757 561.5	−1.2	838 603.8	−0.2	1 074 920.4	−0.0
3 2	765 612.1	−0.0	847 103.8	0.2	1 083 261.0	−0.1
4 3	773 482.9	0.2	855 576.1	0.8	1 091 518.0	−1.5
5 4	781 170.6	1.4	864 014.2	−0.0		
6 5	788 665.9	0.2	872 415.6	0.1	1 107 765.3	−0.6
7 6	795 966.0	0.1	880 774.6	1.0	1 115 740.1	−0.3
8 7					1 123 604.7	−0.7
B'' (MHz)	4280.838(42)					
D_J'' (kHz)	110.61(54)					
ν_0 (MHz)	740 944.81(40)		821 536.32(41)		1 058 010.90(43)	
B' (MHz)	4197.344(46)		4272.264(44)		4245.975(48)	
D_J' (kHz)	137.16(59)		130.56(55)		141.92(58)	

centrifugal distortion constant D_J and the large residuals of the fit. The Δ upper state of the second band is split, and the component of same parity with respect to the Σ state is more weakly perturbed than the other parity component. As will be discussed in detail below, these states should be of F symmetry, and the Π lower state should be perturbed by a Σ state lying below it. In addition, because the l-type doubling constant is positive, we can infer that the upper Σ state and the perturbing Σ state should have opposite parity.

The last two VRT transitions at 28.16 and 30.66 cm^{-1} [$(A/F)_5$ and $(A/F)_8$, respectively] are both $\Pi \leftarrow \Sigma$ bands, and for both Π upper states the q constant is positive, indicating that the perturbing state is either of opposite parity to the Σ state and below the Π state, or that it is of the same parity of the Σ state and above the Π state. For the 28.16 cm^{-1} band, we can infer that the latter case is true; the perturbing state must be above, since the lower energy parity component of the Π state is actually perturbed, as evidenced by the negative value of the centrifugal distortion constant (i.e., $D_J - q_D$).

For all these bands, the rotational constants are only 0.3%–3% smaller in the upper states than the lower states, minimizing the possibility that these spectra correspond to intermolecular stretching vibrations of the cluster. For example, in the case of Ar–H_2O the change in the upper states of the stretching bands is larger than 5%.[5]

C. Interpretation of the spectrum

As previously mentioned, the CH_4–H_2O complex might be expected to have a similar VRT energy level structure to that of the Ar–H_2O complex. In fact the lowest nonvanishing multipole moment of CH_4 is the octopole, and the enhanced role of the electrostatic contribution in CH_4–H_2O relative to Ar–H_2O should be responsible for the difference between the anisotropy of the two clusters, as reported by Szczęśniak *et al.*[15]

We shall describe the VRT spectrum of CH_4–H_2O as that of two weakly coupled free internal rotors. The angular momentum of each rotor will be independently coupled to the cluster frame, but the two rotors will only weakly couple to each other. If the electrostatic contribution in CH_4–H_2O, which includes high order multipole interactions and charge overlap effects,[15] do not drastically change the Ar–H_2O-like interactions, then the spectrum would be expected to display many transitions near 21 and 37 cm^{-1}. Near 21 cm^{-1}, these would correspond to differ-

TABLE VIII. Observed frequencies (MHz), residuals (MHz), and spectroscopic constants from a fit of the $(A/F)_5$ band.

Band $J' \leftarrow J''$	$(A/F)_5$ Observed	O–C
	$\Pi \leftarrow \Sigma$	
7 8	771 799.3	0.1
6 7	781 395.8	−0.0
5 6	790 834.6	−0.4
4 5	800 119.9	0.2
3 4	809 248.6	−0.5
2 3	818 220.6	0.1
1 2	827 031.4	1.0
1 1	844 268.9	−0.4
2 2	844 500.0	−0.3
3 3	844 841.7	−0.4
4 4	845 289.8	0.5
5 5	845 835.2	0.3
6 6	846 470.0	−0.4
7 7	847 186.4	0.1
1 0	852 462.1	0.1
2 1	860 602.5	−0.3
3 2	868 576.0	−0.4
4 3	876 384.3	0.3
5 4	884 027.1	0.9
6 5	891 501.0	−0.5
B'' (MHz)	4238.891(51)	
D_J'' (kHz)	47.16(77)	
ν_0 (MHz)	844 152.85(40)	
B' (MHz)	4225.912(82)	
D_J' (kHz)	58.5(31)	
H_J' (Hz)	−199.(37)	
q' (MHz)	142.700(79)	
q_D' (kHz)	134.7(43)	
q_H' (Hz)	528.(56)	

ent free internal rotation states of methane superimposed upon a transition analogous to the $n=0$, $\Pi(1_{10}) \leftarrow \Sigma(1_{01})$ transition of ortho Ar–H_2O, and the group near 37 cm^{-1} would be analogous to the $n=0$, $\Pi(1_{11}) \leftarrow \Sigma(0_{00})$ transition of para Ar–H_2O.

Since we do, in fact, observe a dense spectrum in the region 18–19 cm^{-1}, as well as several bands spread in the region 25–35 cm^{-1} but mainly concentrated around 30 cm^{-1}, we have assigned as ortho states those involved in the low frequency bands, and as para states those observed at higher frequency.

We have been able to unambiguously assign the states of E symmetry as discussed above. In an attempt to determine the symmetry of the remaining energy levels we can exploit, at least for the para lower states, the energy correlation diagram reported by Ohshima and Endo in their paper on CH_4–HCl.[13]

These authors studied the internal rotation of methane in the complex, assuming the HCl is positioned with the hydrogen atom pointing towards a face-center of the CH_4 tetrahedron. With this geometry there are four equivalent configurations, leading to a fourfold degeneracy for each energy level in the absence of internal rotation. This degeneracy is partially removed when tunneling between the four minima occurs because of the low potential energy barrier to the internal rotation of CH_4. The reported correlation diagram for the complex energy levels as a function of the lowest-order anisotropic term, V_3, shows that a pair of Σ states of A and F symmetry, and an E symmetry Π state can be populated in a 5 K molecular beam. An additional F symmetry Π state can also be significantly populated depending on the value of the V_3 anisotropic term, since the two F symmetry states get closer in energy as V_3 becomes smaller. Thus, for states correlating to the 0_{00} para ground state of water, these considerations lead us to expect one E symmetry Π state, two Σ states (one of A and one of F symmetry), and possibly, one F symmetry Π state.

In Table XI the spectroscopic constants of the observed lower states are reported. The states are labeled by their Ω quantum number and a progressive index [which corresponds to the order, from left to right, of the lower states presented in Figs. 1(a) and 1(b)], for identification purposes the VRT bands originating from each state are reported in the rightmost column. For the two Π states of A/F symmetry, the rotational and centrifugal distortion constants for each parity component are reported. Among the lower levels assigned as correlating to the 0_{00} para ground state of water, we observe, in fact, a Π state of E symmetry (#5 of Table XI), and two Σ (#6, 8), and one Π (#7) states of A/F symmetry. This observation substantiates the assignment and allows us to assign the #7 Π state as having F symmetry. The question then arises about which Σ state is the A symmetry ground state and which one is the F symmetry state.

The force constants computed from the rotational and centrifugal distortion constants in the pseudodiatomic approximation (see next section) are 3.59 N/m for state #6, and 1.52 N/m for #8. A comparison to the force constant values of CH_4–HX type clusters[12] reported in Table XII suggests that the 3.59 N/m value is too high, while the 1.52 N/m value compares well to the force constants of these CH_4 containing clusters which exhibit methane internal rotation. The unrealistic force constant derived from state #6 is most likely due to the effects of Coriolis coupling, which are not expected to be significant for the relatively isolated A^+ Σ state.

Thus, assuming state #8 is the para ground state, then state #6 would be a para state of F symmetry perturbed by the nearby F symmetry Π state (#7b). This picture is confirmed by considering the mean value of D_J for the two perturbing states. It is found that this value of 124.33 kHz is very close to the D_J value for the unperturbed component of the Π state (#7a). This is characteristic of a Coriolis interaction occurring between two states.[11] In addition the #2a, 4, 7a states have spectroscopic constants similar to those of the ground state, indicating that these relatively unperturbed states sample the same radial region. The mean value of R_{cm} for states #2a, 4, and 7a is 3.701(2) Å, compared to 3.7024 Å in the ground state. The ortho states #2b Π and #3 Σ behave like the pair of states assigned to F^+ symmetry; again the mean value of D_J for these two states (112.81 kHz) is close to that for the unperturbed Π state (#2a) suggesting that they interact

TABLE IX. Observed frequencies (MHz), residuals (MHz), and spectroscopic constants from fits of the $(A/F)_6$ and $(A/F)_7$ bands.

Bands $J' \leftarrow J''$	$(A/F)_6$		$(A/F)_7$			
	Observed	O–C	Observed	O–C	Observed	O–C
	$\Sigma \leftarrow \Pi$				$\Delta \leftarrow \Pi$	
9 10	813 710.5	−14.6	819 217.4	−0.1		
8 9	823 743.0	−18.4	829 011.3	0.2		
7 8	833 609.9	−9.3	838 750.0	−0.1		
6 7	843 305.8	4.5				
5 6	852 831.7	16.1	858 008.6	0.0		
4 5	862 188.2	15.3	867 497.9	−0.1		
3 4	871 391.4	6.4	876 874.8	0.5	877 813.3	0.0
2 3	880 455.8	−6.8	886 123.7	−0.1	886 683.5	0.0
1 2	889 393.8	−20.5				
14 14			906 495.2	0.0		
13 13			907 364.3	0.1		
12 12			908 155.9	0.0		
11 11			908 879.3	−0.8		
10 10			909 543.9	0.6		
9 9			910 149.8	0.4		
8 8			910 700.0	−0.2		
7 7	900 690.2	−8.0	911 196.4	0.3	909 377.9	0.0
6 6	902 302.9	5.7	911 635.6	−0.7	910 149.8	−0.4
5 5	903 668.5	15.4	912 018.9	−0.1	910 869.3	0.7
4 4	904 785.5	15.8	912 342.1	−0.3	911 519.0	−0.4
3 3	905 660.8	8.1	912 604.3	0.0	912 080.5	−0.5
2 2	906 302.4	−5.9	912 803.3	0.6	912 529.1	−0.2
1 1	906 722.4	−19.5				
2 1	924 003.8	−5.8	930 130.4	0.1	930 230.6	0.0
3 2	932 339.1	7.5				
4 3			946 609.8	−0.3		
5 4	948 513.0	15.5	954 615.6	−0.2	955 714.2	1.2
6 5	956 313.5	5.8	962 473.8	0.0	964 159.7	−1.0
7 6	963 906.0	−7.6	970 192.2	0.1	972 593.7	0.3
8 7	971 285.1	−16.3	977 779.9	0.7		
9 8	978 447.3	−14.9	985 243.1	−0.2		
10 9	985 396.0	1.0	992 590.7	−0.5		
11 10	992 132.4	22.9	999 827.9	0.2		
12 11	998 658.0	28.3				
13 12	1 004 976.2	−20.8				
B'' (MHz)	4 379.882[a]				4379.882(38)	
D_J'' (kHz)	157.94[a]				157.94(69)	
H_J'' (Hz)	39.9[a]				39.9(36)	
q'' (MHz)	47.145[a]				47.145(18)	
q_D'' (kHz)	87.08[a]				87.08(49)	
q_H'' (Hz)	103.9[a]				103.9(32)	
ν_0 (MHz)	906 957.6(7.1)				913 002.86(29)	
B' (MHz)	4 295.79(0.44)				4 322.538(51)	
D_J' (kHz)	295.1(66)				−45.7(15)	
H_J' (Hz)	45.4(26)				−775(16)	
q' (MHz)					0.498(49)	
q_D' (kHz)					267.6(25)	
q_H' (Hz)					1391(30)	

[a]Fixed to the value obtained by fitting the $\Delta \leftarrow \Pi$ band, see text.

via Coriolis effect, which requires that they have the same symmetry. If we correct the rotational constants of the #3 and #6 Σ states, which are pushed down in energy by interaction with the #2b and #7b Π states lying above them, respectively, by the value of the q constant of the corresponding perturbing Π state, we can observe that the #1 and #5 E symmetry Π states and these two Σ states (#3 and #6) sample a region of the potential surface having $R_{cm}=3.730(2)$ Å.

In previously studied CH_4 containing clusters,[9–13] the rotational constants vary only slightly with the methane internal-rotation states, suggesting that the same radial region is sampled. In CH_4–H_2O, on the other hand, the methane internal-rotation states seem to sample two different radial regions, in the same way for ortho and para states. This is most likely due to angular-radial coupling.

The observation, reported above, that ortho states #2 Π and #3 Σ should have the same symmetry suggests an

TABLE X. Observed frequencies (MHz), residuals (MHz), and spectroscopic constants from a fit of the $(A/F)_8$ band.

Band $J' \leftarrow J''$		$(A/F)_8$ Observed	O–C
		$\Pi \leftarrow \Sigma$	
7	8	845 616.2	0.5
6	7	855 272.8	−0.7
3	4	883 477.9	−0.1
2	3	892 608.4	0.2
1	2	901 595.6	−0.5
1	1	919 166.0	0.9
2	2	919 232.4	−0.4
3	3	919 333.8	−0.9
4	4	919 472.1	0.9
5	5	919 641.8	−0.8
6	6	919 850.5	0.6
7	7	920 094.4	0.8
8	8	920 374.4	−0.4
9	9	920 694.4	−0.2
10	10	921 054.1	−0.2
11	11	921 455.3	−0.1
12	12	921 899.6	0.0
13	13	922 388.7	0.0
14	14	922 925.0	0.1
15	15	923 510.7	0.1
16	16	924 148.5	−0.0
17	17	924 841.4	−0.1
18	18	925 592.9	−0.0
19	19	926 406.4	0.1
1	0	927 673.3	0.7
2	1	936 059.3	−0.0
3	2	944 289.9	0.1
4	3	952 360.9	0.3
5	4	960 270.1	−1.4
6	5	968 019.7	−1.0
7	6	975 606.8	−0.2
8	7	983 030.5	0.5
9	8	990 289.7	0.7
10	9	997 385.5	1.2
11	10	1 004 314.8	−1.2
B'' (MHz)		4346.806(55)	
D_J'' (kHz)		120.53(57)	
H_J'' (Hz)		−1.94(12)	
ν_0 (MHz)		919 131.34(26)	
B' (MHz)		4317.263(50)	
D_J' (kHz)		111.55(47)	
q' (MHz)		92.855(17)	
q_D' (kHz)		7.54(23)	

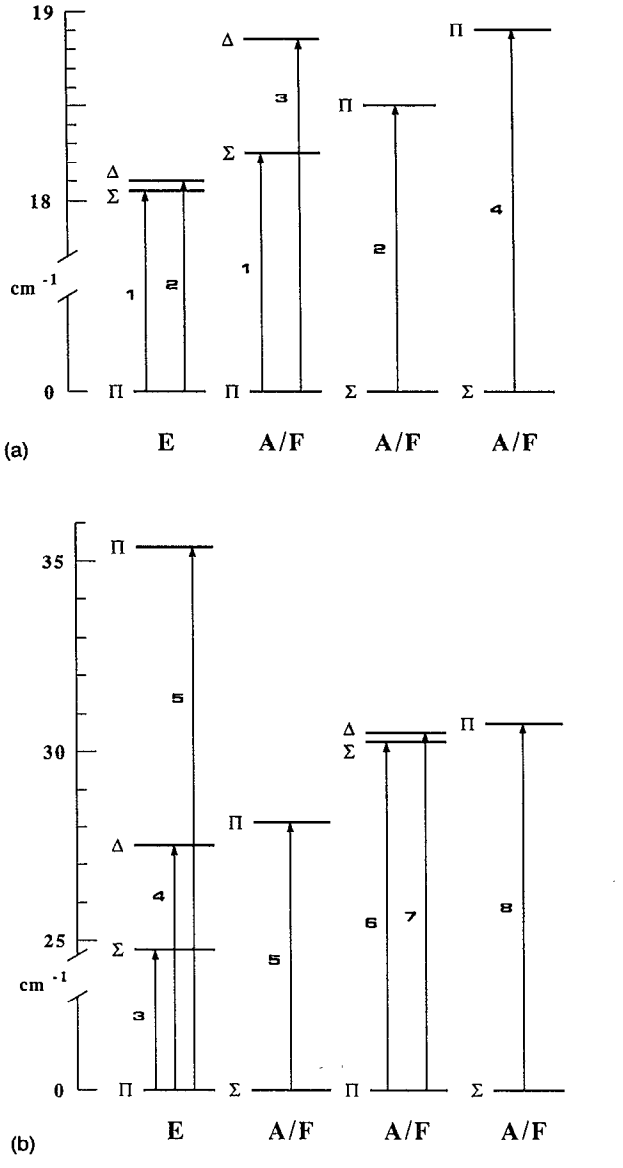

FIG. 1. Overview of the observed VRT bands of CH_4–H_2O. The observed states are grouped as having either (a) ortho or (b) para water symmetry. Methane symmetry labels are reported at the bottom of the diagrams, and a number labels different bands with the same symmetry.

assignment for these states. We have assumed that the observed ortho bands connect states correlating to the $1_{0,1}$ level of H_2O to states correlating to the $1_{1,0}$ level, and we are in the hypothesis of CH_4 and H_2O being weakly coupled internal rotors. Therefore we cannot observe any Δ state of A symmetry, since the observed A symmetry states should correlate to the $j=0$ methane function (as the $j=3$ function is much higher in energy) and $\Omega \leqslant 1$. We have, in fact, observed a VRT band connecting the #2 Π state to a Δ state [$(A/F)_3$], indicating that these are not A symmetry states. Therefore, the two interacting Σ and Π ortho states (#3 and #2) should be assigned to F^- symmetry, and the last unassigned ortho state (#4 Σ) has to be assigned to A^- symmetry. The same argument applies to the para states, since they correlate to the 0_{00} and 1_{11} levels of H_2O, thus confirming the previous assignment. The #7 Π state assigned to F^+ symmetry is in fact connected to a Δ state [$(A/F)_7$ band].

Even though the assignment given above is supported by several convincing arguments, it nevertheless must be considered somewhat tentative. Additional spectroscopic data will be required to resolve remaining questions regarding the complicated nature of the VRT states for this cluster.

D. Pseudodiatomic potential

Within the pseudodiatomic approximation, the average center of mass separation R_{cm}, the force constant k_s, and the harmonic frequency ω_s for the vdW stretching are expressed as

TABLE XI. Rotational and centrifugal distortion constants for the observed lower states. The leftmost column is a progressive index that corresponds to the order, from left to right, of the states presented in Figs. 1(a) and 1(b). The rightmost column shows the VRT bands originating from each state.

	State	B(MHz)	D_J(kHz)	Symmetry[a]	Bands
			ortho states		
1	Π	4277.222	105.56	E^-	$(E)_1$, $(E)_2$
2a	Π	4350.149	107.86	F^-	$(A/F)_1$, $(A/F)_3$
2b	Π	4380.301	156.04	F^-	$(A/F)_1$, $(A/F)_3$
3	Σ	4252.899	69.58	F^-	$(A/F)_2$
4	Σ	4345.533	111.45	A^-	$(A/F)_4$
			para states		
5	Π	4280.838	110.61	E^+	$(E)_3$, $(E)_4$, $(E)_5$
6	Σ	4238.891	47.16	F^+	$(A/F)_5$
7a	Π	4356.308	114.39	F^+	$(A/F)_6$, $(A/F)_7$
7b	Π	4403.454	201.50	F^+	$(A/F)_6$, $(A/F)_7$
8	Σ	4346.806	120.53	A^+	$(A/F)_8$

[a]Tentative assignment. See text.

$$R_{cm}=(h/8\pi^2 B\mu)^{1/2}, \tag{2a}$$

$$\omega_s=(4B^3/D_J)^{1/2}, \tag{2b}$$

$$k_s=(4\pi)^2\mu B^3/D_J. \tag{2c}$$

Here, μ is the pseudodiatomic reduced mass of the complex, h is Planck's constant, and B and D_J are the rotation and distortion constants, respectively.

The spectroscopic constants of the state assigned as the ground state (Σ A^+) yield the following values: R_{cm} =3.7024 Å, ω_s=55 cm^{-1}, k_s=1.52 N/m. At the same level of approximation the following values are reported[23] for Ar–H_2O: R_{cm}=3.6908 Å, ω_s=35.1 cm^{-1}, k_s=0.902 N/m. Having a very similar vdW bond length, the larger force constant of the CH_4–H_2O indicates that it is more strongly bound than Ar–H_2O. The harmonic stretching frequency is likely to be overestimated by ~10–20%, as suggested by experience with other clusters, but this value confirms that the VRT bands reported here, all of them below 35.5 cm^{-1}, are not intermolecular stretching bands.

V. DYNAMICAL CALCULATIONS

Because of the difficulties in interpreting the complicated spectral pattern observed, we have estimated the VRT energy level pattern by calculation of the angular Hamiltonian in a basis set which is most appropriate for strong coupling of the water and methane internal angular momenta to the cluster frame. The IPS that we have employed is a spherical expansion of the *ab initio* surface reported by Woon *et al.*,[17] which was the only full surface available when this work was in progress.

TABLE XII. Force constants for some CH_4–HX clusters.[a]

X	Cl	Br	CN
k_s (N/m)	2.165	1.876	1.587

[a]Reference 12.

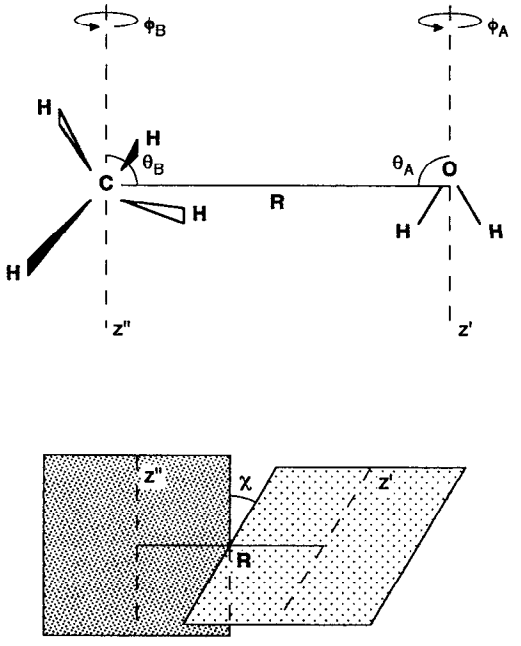

FIG. 2. The Jacobi coordinate system for the intermolecular degrees of freedom of the methane–water complex.

A. Computational methods

The dynamical calculations used to determine the VRT energies involve solving the Schrödinger equation for the internal motions of monomers on a six-dimensional IPS. Brocks *et al.*[24] have derived a Hamiltonian and the matrix elements in the angular basis for the general interaction of two polyatomic species. Our initial statement of the problem closely follows their prescription, and the subsequent calculations of VRT dynamics in the ammonia dimer done by van Bladel *et al.*[25]

The coordinate system employed for the interaction of methane with water, shown in Fig. 2, is a generalized Jacobi coordinate system with the origin at the H_2O (denoted molecule A in many of the equations) center of mass, and with R being a vector from this origin to the center of mass of the CH_4 molecule (denoted B). The (right handed) internal frames chosen for the subunits are as follows: for H_2O the z'-axis is along the symmetry axis and the x'-axis is in the plane of the molecule; for CH_4 we orient the molecule such that the hydrogens are at positions $(r_{x''},r_{y''},r_{z''})=(1,1,1),(-1,-1,1),(-1,1,-1)$, and $(1,-1,-1)$. The x'', y'', and z'' axes each bisect two HCH angles. The coordinates of the internal frames relative to the body-fixed frame are chosen such that θ_B is the angle between the CH_4 z''-axis and the vector R, and ϕ_B describes the rotation of methane about this axis, with ϕ_B=0 when x''-axis is coplanar with R and z''. The angle θ_A is the angle between the H_2O symmetry axis and R, and ϕ_A describes the rotation of water subunit about this symmetry axis, with ϕ_A=0 when the x'-axis is coplanar with R and z'. The final angle necessary to fully specify the geometry of the interacting pair is $\chi=\chi_A-\chi_B$ (we can assume χ_B

$=0$), a dihedral angle which specifies the relative angle between the two molecule-fixed z-axes.

The Hamiltonian for the interaction of CH_4 and H_2O, averaged over the respective monomer ground vibrational states, is

$$H=\frac{-\hbar^2}{2\mu R}\frac{\partial^2}{\partial R^2}R+\frac{\hbar^2}{2\mu R^2}(\hat{J}^2+\hat{j}^2-2\hat{j}\cdot\hat{J})+H_A+H_B + V(R,\chi_A,\theta_A,\phi_A,\chi_B,\theta_B,\phi_B), \quad (3)$$

where μ is the pseudodiatomic reduced mass, j is the sum of the rotational angular momenta of each of the two monomers, and J is the total angular momentum of the system. The vibrationally averaged monomer Hamiltonians, H_A and H_B, are both of the form

$$H=B_x\hat{j}_x^{m2}+B_y\hat{j}_y^{m2}+B_z\hat{j}_z^{m2}. \quad (4)$$

The superscript m is used to refer to operators written in the body-fixed Cartesian frame of the monomer. The monomer Hamiltonians reduce to the usual spherical rotor and asymmetric rotor expressions for CH_4 and H_2O, respectively. The Coriolis operator $-2\hat{j}\cdot\hat{J}$ is expressed as

$$-2\hat{j}\cdot\hat{J}=-2\hat{j}_z\hat{J}_z-2\hat{j}_+\hat{J}_+-2\hat{j}_-\hat{J}_-, \quad (5)$$

where

$$\hat{j}_\pm=\hat{j}_x\mp\hat{j}_y,\quad \hat{J}_\pm=\hat{J}_x\pm\hat{J}_y.$$

We expand the trial wave function in a complete angular basis

$$\sum_{\Omega_A,\Omega_B} D^{(j_A)*}_{\Omega_A k_A}(\chi_A,\theta_A,\phi_A)\,D^{(j_B)*}_{\Omega_B k_B}(\chi_B,\theta_B,\phi_B) \times\langle j_A\Omega_A j_B\Omega_B|j\Omega\rangle\, D^{(J)*}_{M\Omega}(\alpha,\beta,0), \quad (6)$$

where $D^{(j)*}_{\Omega k}(\gamma,\beta,\alpha)$ is a normalized Wigner rotation matrix in the phase convention of Condon and Shortley, and the quantity in angle brackets is a Clebsh–Gordon coefficient. Matrix elements of the kinetic energy operators in this basis are given by Brocks *et al.*[24]

To reduce the order of the Hamiltonian matrix, linear combinations of the primitive basis of Eq. (6) are taken which transform as irreducible representations of molecular symmetry group G_{48}. The Wigner D-matrices which represent internal rotation of the methane are symmetrized to give functions of A_1^+, A_2^+, E^+, F_1^+, and F_2^+ symmetry under G_{48}. They are tabulated by Smith and Secrest[26] through $j=8$ in the $T(M)$ group, which has the symmetries A, E, and F. The subscript 1 and 2 are assigned using the intermolecular potential as a ladder up the rotational manifold. The potential energy operator only connects states of the same symmetry. Starting with the function $|0_0\rangle$, $\Gamma=A_1$, $|3_2\rangle-|3_{-2}\rangle$, $\Gamma=A_2$, the rest of the eigenfunctions may be assigned a definite parity. Internal rotor functions for water are the usual Wang combinations of symmetric rotor functions. They transform as A_1 and A_2 (k=even, para), B_1 and B_2 (k=odd, ortho), under the V group of the asymmetric rotor Hamiltonian, and as A_1^+, A_2^+ and A_1^-, A_2^-, respectively, under G_{48}. Finally, parity adapted eigenfunctions for the A and F representations are generated by taking positive ($\epsilon=0$) and negative ($\epsilon=1$) linear combinations of functions with $|\Omega|\rangle 0$. Overall rotation functions with $(-1)^{(J-j+\epsilon)}=1$ transform as A_1^+ and functions with $(-1)^{(J-j+\epsilon)}=-1$ transform as A_1^-. The symmetry of the total rovibrational wave function is the direct product of the symmetry of the component functions. The Hamiltonian does not couple states of different overall symmetry with respect to G_{48}.

In these dynamical calculations we employ two approximations in order to make the numerical calculations possible with the available computer resources, the reversed adiabatic approximation (RAA), and the helicity decoupling approximation. In the RAA we assume that the effective radial potential which is sampled by the bending VRT states of interest is the same for all of these states. For this to be true, this effective angular potential must average over the radial wave function in exactly the same way for all of the bending states of interest. In other words, the angular-radial coupling must not vary from state to state. The IPS which we consider will be then an effective five-dimensional angular surface, and not the full six-dimensional surface described above. This simplifies consideration of the form of the potential considerably, since we are then able to replace all functions of R by numbers which correspond to the effective radial matrix elements. The helicity decoupling approximation involves the neglect of the Coriolis terms ($J_\pm$,$j_\pm$) which split the otherwise degenerate pairs of $A_{1/2}$ and $F_{1/2}$ levels in states with $\Omega>0$. These terms are observed to be in the range 0.001–0.005 cm^{-1} in the experimental spectrum. In this approximation, the body fixed projection Ω is a good quantum number.

The Hamiltonian was evaluated for $J=2$ with a basis set determined by $j_A^{max}=4$, $j_B^{max}=7$, $j^{max}=8$, which was sufficient to converge the lowest energy levels to an accuracy better than 0.5 cm^{-1}. The calculations were performed on a CRAY-XMP/14.

B. The intermolecular potential energy surface

Woon *et al.*[17] employed *ab initio* Hartree–Fock and second order many-body perturbation theory to generate data for the pair potential of CH_4–H_2O. They then fit 33 points to an atom–atom potential including exponential repulsion, R^{-6} and electrostatic attraction as interaction terms. Few *ab initio* points were used, since they were sufficient to describe the region near the minimum; this treatment may very well be inadequate for our case, as the VRT states accessed by our spectra sample a very large region of coordinate space. Another weakness of this surface is the disagreement between its global minimum, which occurs at a geometry with a methane hydrogen pointing toward the water oxygen, and that reported by Szczęśniak *et al.*,[15] where their higher level *ab initio* calculations find the minimum energy with a water hydrogen pointing toward a face-center of the methane tetrahedron.

The atom–atom potential has been expanded in a complete set of orthogonal angular functions for use in the calculation of the VRT energy levels,

$$V_{\rm int}(R,\chi_A,\theta_A,\phi_A,\chi_B,\theta_B,\phi_B)$$
$$=\Sigma_\Lambda V_\Lambda(R)A_\Lambda(\chi_A,\theta_A,\phi_A,\chi_B,\theta_B,\phi_B), \quad (7)$$
$$A_\Lambda=8\pi^2(2L+1)^{1/2}\Sigma_M\begin{pmatrix}L_A & L_B & L\\ M & -M & 0\end{pmatrix},$$
$$D^{(L_A)^*}_{MK}(\chi_A,\theta_A,\phi_A)D^{(L_B)^*}_{-MK}(\chi_B,\theta_B,\phi_B),$$

where Λ refers to the set of quantum numbers (L_A,K_A,L_B,K_B,L). The matrix elements of the angular potential have been derived by Brocks *et al.*[24]

Since the angular functions form an orthogonal set, the V_Λ dynamic coefficients for the atom–atom potential can be calculated by integrating over all angular coordinates.[25] We have used a 14 point Gauss–Legendre quadrature for polar angles θ_A and θ_B on the interval $[0,\pi]$, a 12 point Gauss–Chebyschev quadrature for dihedral angle χ on the interval $[0,2\pi]$, and a 10 point Gauss–Chebyschev quadrature for azimuthal angles ϕ_A and ϕ_B on the interval $[0,\pi]$. The following constraints have been used in order to reduce the number of coefficients to be computed.[27]

$$V_{L_AK_AL_BK_BL}=(-)^{L_A+K_A+L_A+K_B+L}V_{L_A-K_AL_B-K_BL} \quad (8a)$$

since V is real;

$$V_{L_AK_AL_BK_BL}=(-)^{K_A}V_{L_A-K_AL_BK_BL} \quad (8b)$$

with K_A even, due to H_2O symmetry;

$$V_{L_AK_AL_BK_BL}=(-)^{L_B}V_{L_AK_AL_B-K_BL} \quad (8c)$$

with K_B spaced by 4, due to CH_4 symmetry;

$$L_A+L_B+L \text{ even.} \quad (8d)$$

If we truncate the expansion of Eq. (7) at $L_B=6$ and $L_A=5$, and only coefficients greater than 0.6 cm^{-1} are considered, the truncated potential reproduces the atom–atom potential to $\sim 5\%$. The calculations are performed with R fixed at 3.89 Å, the value at which the site–site potential exhibits the global minimum.

C. Results

Figures 3(a) and 3(b) show the energy level diagram for $J=2$ para and ortho states, as obtained from the calculations. The methane symmetry labels are reported at the bottom of the diagrams, the capital Greek letter at the left of each level refers to the vibrational angular momentum Ω, and the sign in front of the Σ states refers to their parity. The numbers at the right of each level are the rotational states of the methane and water monomers to which the level mainly correlates. Even if a state is the result of the mixing of several basis functions, it is still possible to relate it to a methane and water basis state in order to determine which CH_4–H_2O transitions should correlate to the H_2O transitions of interest, assuming the propensity rule $\Delta j_{CH_4}=0$.

The pattern of the lower para states supports the results obtained by Ohshima and Endo;[13] we have an A symmetry Σ state, an E symmetry Π state, and two E symmetry states, Σ and Π with the former lying below the latter. Consider now the VRT transitions related to the $1_{11}\leftarrow 0_{00}$ water transition. The A symmetry $\Pi\leftarrow\Sigma$ band is predicted at 37 cm^{-1}, and the presence of a Σ state above the Π state with the same parity of the ground state is in agreement with the positive value of the l-type doubling constant observed for the upper state in the $(A/F)_8$ band. But the predicted frequency is too high with respect to the observed frequency of 30.66 cm^{-1}. The F symmetry $\Sigma\leftarrow\Pi$ and $\Delta\leftarrow\Pi$ bands are also predicted too high in frequency [35 and 37 cm^{-1} compared to 30.25 and 30.45 cm^{-1} mea-

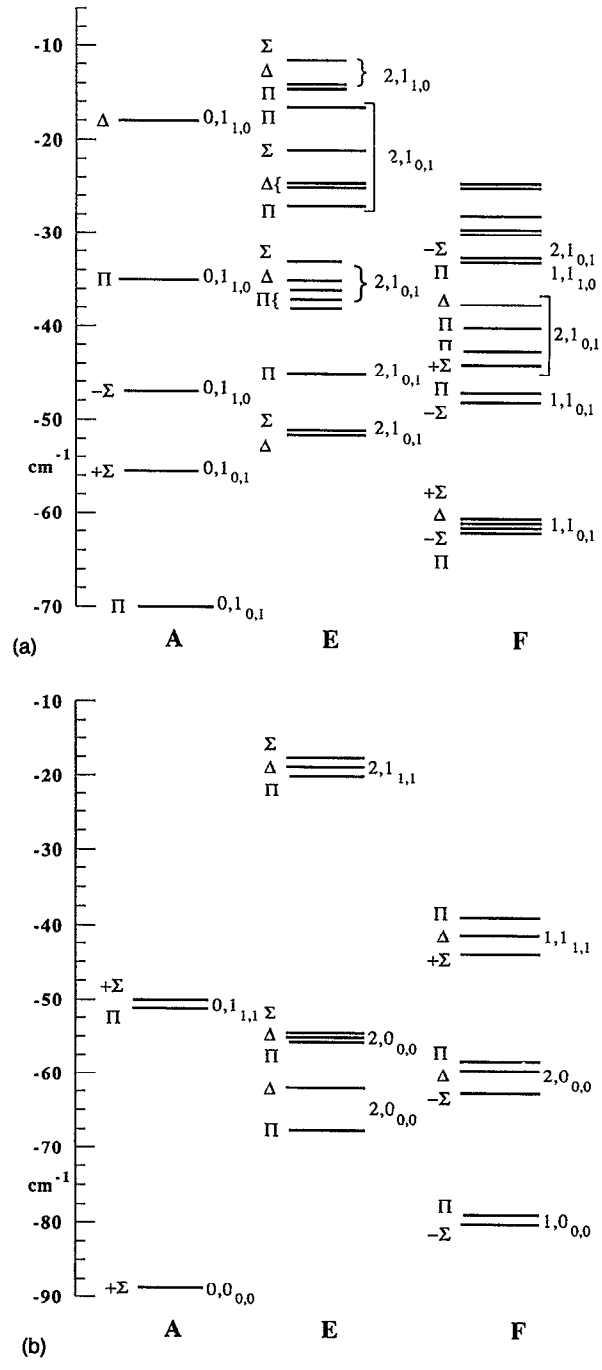

FIG. 3. Computed energy level diagram for $J=2$ (a) ortho and (b) para states of CH_4–H_2O.

sured in bands $(A/F)_6$ and $(A/F)_7$]. In addition, the F symmetry Π upper state is predicted to lie above the Σ and Δ states, in contrast with the $(A/F)_6$ $\Pi \leftarrow \Sigma$ band observed at 28.16 cm^{-1}. The agreement between the calculated and experimental results is even worse for the E symmetry case; the $\Pi \rightarrow \Pi$, Δ, Σ transitions are predicted in the range 47–50 cm^{-1}, with the upper levels closely spaced and in the order shown. This is in sharp contrast with the observation of the Σ state 2.7 cm^{-1} below the Δ state, which is in turn 7.9 cm^{-1} below the Π state.

The computed energy level diagram of the ortho states is very dense, and it is impossible to determine the correlation between observed bands and predicted bands, as described above for the para states. The pattern of the lower states does not agree with the observed ordering, and, with the exception of an A symmetry $\Sigma \leftarrow \Pi$ band at 23 cm^{-1}, all the transitions correlating to the $1_{10} \leftarrow 1_{01}$ water transition are predicted to occur above 30 cm^{-1}.

Unfortunately, the reported calculations are inconclusive, and no one of our assignments can be confirmed in terms of the results. A major inconsistency is that there is no evidence for a concentration of the ortho transitions at frequencies lower than the para bands; the ortho bands are not predicted to occur below 30 cm^{-1}.

The most probable reason for this failure is the inadequacy of the atom–atom potential, which has been optimized only in the minimum region. In addition, this potential is likely to improperly locate the global minimum, as already discussed. Of course, an obvious deficiency of this calculation is the use of the RAA, required here by the limits of available computer facilities. We have in fact observed evidence for angular radial coupling, and perhaps we cannot confine the calculations to the angular degrees of freedom alone, but must include the radial coordinate explicitly. Future dynamical calculations must address these problems in hopes of successfully obtaining the energy level diagram for the methane–water complex from a first principles calculation.

VI. CONCLUSIONS

Extensive measurements in the FIR region from 18 to 35.5 cm^{-1} have been performed for the methane–water dimer with the use of tunable laser techniques, leading to the rotational assignment of thirteen VRT bands. By analogy to the argon–water cluster and relying on a published study on the methane internal rotation in CH_4–HCl complex,[13] an interpretation of the spectrum has been proposed. The basic hypothesis of this interpretation is that the anisotropy of the intermolecular potential is fairly weak, and the monomers undergo hindered rotations within the complex. Therefore, the VRT energy levels of the dimer will correlate strongly with the rotational levels of each monomer, leading to para and ortho nuclear spin conformers of A, F, and E symmetry.

In the framework of this hypothesis, dynamical calculations in a basis set of free rotor functions have been performed employing an analytical *ab initio* potential.[17] Even though the agreement between the predicted and the observed VRT transitions is not entirely satisfactory, these calculations support out the assignment of the lower para states, and the hypothesis of low anisotropy. Since the weakest aspect of our dynamical calculations is the *ab initio* site–site potential employed, a more reliable analytical surface, such as that reported by Szczęśniak *et al.*,[15] will enable us to compute a VRT energy level diagram in better agreement with the experimental observations. However, the RAA treatment may force some inconsistencies as well. Clearly, a full six-dimensional treatment of the VRT dynamics would be preferable.

The experimental data can give considerable insight into the nature of the IPS. For instance assignment of bands sharing a common F symmetry para upper state would lead to the determination of the energy separation of the Σ and Π states labeled #6 and #7 above, thus allowing an estimate of the lowest-order anisotropic term relative to the methane subunit (V_{00323}). However, many terms in the series expansion of the potential are important, and they will ultimately be required to accurately describe the forces in all six dimensions in the range of configuration space sampled by the bound vibrational levels. In any case, it is clear that high resolution FIR spectroscopic data will ultimately provide the means to determine a detailed and accurate six-dimensional IPS, as advances in computational methods and hardware proceed.

Note added in proof. Recent Fourier transform microwave spectroscopy measurements of the hydrogen nuclear hyperfine splittings in CH_4–H_2O[8] confirm our assignment of the water symmetry states and are consistent with our assignment of the methane symmetry states.

ACKNOWLEDGMENTS

We thank Dr. G. T. Fraser and Dr. R. D. Suenram, and Dr. M. Szczęśniak for providing their results before publication. L. D. acknowledges a CNR (Italian National Research Council) fellowship for a period of leave in Berkeley. This work is supported by the Experimental Physical Chemistry Program of the National Science Foundation (Grant No. CHE-9123335).

[1] A. Ben-Naim, *Hydrophobic Interactions* (Plenum, New York, 1980).
[2] P. L. Privelov, S. I. Gill, and K. P. Murphy, Science **250**, 297 (1990).
[3] A. Ben-Naim, J. Chem. Phys. **90**, 7412 (1989).
[4] R. C. Cohen, K. L. Busarow, K. B. Laughlin, G. A. Blake, M. Havenith, Y. T. Lee, and R. J. Saykally, J. Chem. Phys. **89**, 4494 (1988).
[5] R. C. Cohen, K. L. Busarow, Y. T. Lee, and R. J. Saykally, J. Chem. Phys. **92**, 169 (1990).
[6] R. C. Cohen and R. J. Saykally, J. Phys. Chem. **94**, 7991 (1990).
[7] R. C. Cohen and R. J. Saykally, J. Chem. Phys. **95**, 7891 (1991).
[8] G. T. Fraser and R. D. Suenram (private communication).
[9] A. C. Legon, B. P. Roberts, and A. L. Wallwork, Chem. Phys. Lett. **173**, 107 (1990).
[10] A. C. Legon and A. L. Wallwork, J. Chem. Soc. Chem. Commun. **1990**, 590.
[11] A. C. Legon and A. L. Wallwork, J. Chem. Soc. Faraday Trans. **88**, 1 (1992).
[12] M. J. Atkins, A. C. Legon, and A. L. Wallwork, Chem. Phys. Lett. **192**, 368 (1992).
[13] Y. Ohshima and Y. Endo, J. Chem. Phys. **93**, 6256 (1990).
[14] C. A. Schmuttenmaer, R. C. Cohen, J. G. Loeser, and R. J. Saykally, J. Chem. Phys. **95**, 9 (1991).

[15] M. M. Szczęśniak, G. Chalasiński, S. M. Cybulski, and P. Cieplak, J. Chem. Phys. **98**, 3078 (1993).
[16] J. J. Novoa, B. Tarron, M. H. Whangbo, and J. M. Williams, J. Chem. Phys. **95**, 5179 (1991).
[17] D. E. Woon, P. Zeng, and D. R. Beck, J. Chem. Phys. **93**, 7808 (1991).
[18] R. J. Leroy and J. M. Hutson, J. Chem. Phys. **86**, 837 (1987).
[19] J. M. Hutson, Annu. Rev. Phys. Chem. **41**, 123 (1990), and references therein.
[20] G. A. Blake, K. B. Laughlin, R. C. Cohen, K. L. Busarow, C. A. Schmuttenmaer, D. W. Steyert, and R. J. Saykally, Rev. Sci. Instrum. **62**, 1701 (1991).
[21] K. L. Busarow, G. A. Blake, K. B. Laughlin, R. C. Cohen, Y. T. Lee, and R. J. Saykally, J. Chem. Phys. **89**, 1268 (1988).
[22] P. R. Bunker, *Molecular Symmetry and Spectroscopy* (Academic, San Diego, 1979).
[23] G. T. Fraser, F. J. Lovas, R. D. Suenram, and K. Matsumura, J. Mol. Spectrosc. **144**, 97 (1990).
[24] G. Brocks, A. van der Avoird, B. T. Sutcliffe, and J. Tennyson, Mol. Phys. **50**, 1025 (1983).
[25] J. W. I. van Bladel, A. van der Avoird, P. E. S. Wormer, and R. J. Saykally, J. Chem. Phys. **97**, 4750 (1992).
[26] L. N. Smith and D. Secrest, J. Chem. Phys. **74**, 3882 (1981); **91**, 2840 (1989).
[27] C. G. Gray and K. E. Gubbins, *Theory of Molecular Fluids* (Clarendon, Oxford, 1984), Vol. 1.